

AMCoR

Asahikawa Medical University Repository <http://amcor.asahikawa-med.ac.jp/>

The journal of histochemistry and cytochemistry (2012.Aug) 60卷8号:588-602.

A unique ball-shaped Golgi apparatus in the rat pituitary gonadotrope:its functional implications in relation to the arrangement of the microtubule network

Watanabe Tsuyoshi, Sakai Yuko, Koga Daisuke, Bochimoto Hiroshi, Hira Yoshiki, Hosaka Masahiro, Ushiki Tatsuo

Running Headline: BALL-SHAPED GOLGI IN PITUITARY GONADOTROPE

A unique ball-shaped Golgi apparatus in the rat pituitary gonadotrope: its functional implications in relation to the arrangement of the microtubule network

Tsuyoshi Watanabe^{§,*}, Yuko Sakai[§], Daisuke Koga, Hiroki Bochimoto, Yoshiki Hira, Masahiro Hosaka, and Tatsuo Ushiki

Department of Microscopic Anatomy and Cell Biology, Asahikawa Medical University, Asahikawa, Japan (TW, YS, HB, YH); Division of Microscopic Anatomy and Bio-imaging, Department of Cellular Function, Niigata University Graduate School of Medical and Dental Sciences, Niigata, Japan (DK, TU); Laboratory of Molecular Life Sciences, Department of Biotechnology, Akita Prefectural University, Akita, Japan (MH)

[§] These authors contributed equally to this work.

*Correspondence to:
Department of Microscopic Anatomy and Cell Biology,
Asahikawa Medical University,
Midorigaoka-higashi 2-1-1-1,
078-8510 Asahikawa, Japan
Tel.: +81 166 68 2310
Fax: +81 166 68 2319
E-mail: tyshwata@asahikawa-med.ac.jp

Summary

In polarized exocrine cells, the Golgi apparatus is cup-shaped and its convex and concave surfaces are designated as cis and trans faces, functionally confronting the rough endoplasmic reticulum and the cell surface, respectively. To clarify the morphological characteristics of the Golgi apparatus in non-polarized endocrine cells, here we immunocytochemically examined its precise architecture in pituitary gonadotropes, especially in relation to the arrangement of the intracellular microtubule network. The Golgi apparatus in the gonadotropes was not cup-shaped but ball-shaped or spherical, and its outer and inner surfaces were the cis and trans faces, respectively. Centrioles were situated at the center of the Golgi apparatus, from which radiating microtubules isotropically extended to the cell periphery through the gaps in the spherical wall of the Golgi stack. The shape of the Golgi apparatus and the arrangement of microtubules demonstrated in the present study could explain the microtubule-dependent movements of tubulovesicular carriers and granules within the gonadotropes. Furthermore, the spherical shape of the Golgi apparatus possibly reflects the highly symmetrical arrangement of microtubule arrays, as well as the poor polarity in the cell surface of pituitary gonadotropes.

KEY WORDS: Golgi apparatus; Microtubule; Microtubule organizing center (MTOC); Vesicular traffic; Cellular polarity; Endocrine; Anterior pituitary; Gonadotropes; Immunocytochemistry; Electron microscopy.

Introduction

The Golgi apparatus is composed of a stack of cisternae with associated tubulovesicles and functions as a central intersection for intracellular vesicular traffic. During sequential transition in the stacks of the Golgi cisternae, the luminal proteins and lipids are modified by Golgi-resident enzymes, and thereafter they are sorted at the exit site of the Golgi apparatus for destinations such as tubulovesicles toward the cell surface, secretory granules, and lysosomal/endosomal compartments (Griffiths and Simons 1986; Mellman and Simons 1992; Farquhar and Palade 1998; De Matteis and Luini 2008). The overall shape of the Golgi apparatus has been widely accepted as cup-like or hemispherical, based on observations of exocrine cells that secrete a large amount of proteins in a polarized manner. The convex and concave surfaces of the cup-like organization of the Golgi apparatus are designated as the cis and trans faces, which functionally confront the rough endoplasmic reticulum (RER) and the cell surface, respectively (Farquhar and Palade 1981; Mellman and Simons 1992).

Since the architecture and spatial configuration of the Golgi apparatus within cells are possibly involved in its function, its ultrastructure has been examined using various morphological techniques. High voltage transmission electron microscopy (HVTEM) revealed the three-dimensional ultrastructure of the Golgi apparatus in detail, with the aid of a stereogram of a pair of tilted images (Rambourg and Clermont 1990) or computerized tomographic reconstruction (Mogelsvang et al. 2004; Marsh 2005). Alternatively, examination of osmium-macerated specimens with a high resolution scanning electron microscope demonstrated more vividly the three-dimensional images of the Golgi apparatus in various mammalian cells (Tanaka et al. 1986; Koga and Ushiki 2006). These studies not only described its fundamental organization as a ribbon-like structure with compact and non-compact regions (Rambourg and Clermont 1990, 1997) but also revealed the diversity in its three-dimensional architecture in cells/tissues in vivo (Tanaka and Fukudome 1991;

Clermont et al. 1995; Koga and Ushiki 2006).

Besides exocrine cells, endocrine cells also produce and secrete a large amount of peptide hormones and related proteins; hence, their Golgi apparatus is well-developed in general. In the anterior pituitary gland, five distinct subtypes of endocrine cells actively secrete at least six different peptide hormones, namely, luteinizing hormone (LH), follicle stimulating hormone (FSH), thyroid stimulating hormone (TSH), growth hormone (GH), prolactin (PRL), and adrenocorticotrophic hormone (ACTH). Although the configuration of the Golgi apparatus is possibly different from that of exocrine cells and varies depending on the cell types, characteristics in its three-dimensional architecture within the anterior pituitary gland have been overlooked and poorly described.

By scanning electron microscopy, Koga and Ushiki (2006) recently discovered in endocrine cells of the rat anterior pituitary gland a unique ball-like Golgi apparatus, of which the inner surface exhibited ultrastructural characteristics of the trans face. These endocrine cells were seemingly gonadotropes, judging from their oval shape, the size and distribution of secretory granules, and relatively dilated RER. Here we further examined the precise architecture of the Golgi apparatus in pituitary gonadotropes using immunocytochemistry at the light and electron microscopic levels, especially in relation to the arrangement of the microtubule network. The peculiar architecture of the Golgi apparatus observed in gonadotropes may suggest a close relationship between the overall configuration of the Golgi apparatus and the characteristics in the cellular polarity of a typical peptide-secreting endocrine cell. Our findings could also provide an explanation for the intracellular trafficking lines of secretory products within the pituitary gonadotrope.

Materials and Methods

Antibodies

Mouse monoclonal anti-GM130, anti-TGN38, anti-BiP, and anti- γ -adaplin antibodies were purchased from BD Biosciences (San Jose, CA; product codes 610823, 610899, 610978, and 610385, respectively). Additionally, a rabbit polyclonal anti-GM130 antibody (Calbiochem, Nottingham, UK; code CB1008) and a sheep polyclonal anti-TGN38 antibody (AbD Serotec, Oxford, UK; code AHP499G) were used for immunogold labeling and triple immunocytochemical staining at the light microscopic level. Mouse monoclonal and rabbit polyclonal anti- α -tubulin antibodies were purchased from Invitrogen (Carlsbad, CA; code A11126) and Thermo Fisher Scientific Anatomical Pathology (Fremont, CA; code RB-9281-P), respectively. A mouse monoclonal anti-acetylated α -tubulin antibody and mouse monoclonal and rabbit polyclonal anti- γ -tubulin antibodies were purchased from Sigma-Aldrich Co. (St. Louis, MO; codes T7451, T6557, and T3195, respectively). The specificity of these primary antibodies was confirmed by comparing the immunostaining patterns of two different sources of antibodies against each antigen; cryosections of the rat pituitary tissue were simultaneously immunostained with two different antibodies against GM130 [mouse monoclonal (Ms) and rabbit polyclonal (Rb)], TGN38 [mouse monoclonal (Ms) and sheep polyclonal (Sh)], α -tubulin [mouse monoclonal (Ms) and rabbit polyclonal (Rb)], or γ -tubulin [mouse monoclonal (Ms) and rabbit polyclonal (Rb)]. In parallel, the specificity of the antibodies was also confirmed by immunoblotting with extracts of three representative endocrine tissues including pituitary, thyroid, and adrenal glands, as described previously (Sakai et al. 2003). The results of the immunocytochemical analyses and immunoblotting for characterization of the antibodies are summarized in Suppl. Fig. S1.

To identify the endocrine cell types in tissue sections of anterior pituitary glands, rabbit polyclonal anti-ovine LH β (code HAC-OV27(à)-01RBP85), anti-rat prolactin (code

HAC-RT26–01RBP85), anti-rat GH (code HAC-RT25– 01RBP85), and anti-canine TSH antisera were kindly provided by Dr. Matozaki, Gunma University, Japan. Commercially available goat polyclonal anti-LH (Santa Cruz Biotechnology, Santa Cruz, CA; code sc-7824) and rabbit polyclonal anti- ACTH (Sigma-Aldrich; code A1924) antibodies were also used for double or triple immunocytochemical staining at the light microscopic level. Secondary antibodies conjugated with fluorescent dyes (Alexa Fluor 350-, 488-, 594-conjugated donkey polyclonal anti-rabbit-, mouse-, sheep-, goat-IgG) and those with colloidal gold particles (5, 10, 15 nm in diameter) were purchased from Invitrogen and British Biocell International (Cardiff, UK), respectively.

For observations with a laser confocal microscope, biotinylated secondary antibodies (anti-rabbit and goat IgGs; purchased from Vector Laboratories, Burlingame, CA) and Alexa Fluor 405-conjugated streptavidin (Invitrogen) were used for the immunostaining instead of Alexa Fluor 350-conjugated secondary antibodies.

Animals

Twenty male Wistar rats were used for experiments in accordance with the Guide for the Care and Use of Laboratory Animals (Institute of Laboratory Animal Resources, National Research Council, Washington, DC, 1996) under the permission of the experimental animal welfare committee of Asahikawa Medical University (permission 06017). Rats purchased at 6 weeks of age (body weight ~200 g) were housed for 2 weeks in a well-ventilated room (temperature $23 \pm 1^{\circ}\text{C}$; relative humidity 55–65%; lights on between 7:00 AM and 7:00 PM) with food and water ad libitum, and then used for experiments at 8 weeks of age.

Immunofluorescence microscopy

For immunofluorescence microscopy, male rats (n=5) at 8 weeks of age were anesthetized

with ketamine/xylazine (100:10 mg/kg; IM) and then perfused with 30 ml of physiological saline followed by 100 ml of 4% paraformaldehyde (PFA) in 0.1 M phosphate buffer (PB, pH 7.4) containing 3% sucrose. After fixation by perfusion, pituitaries were cut into small pieces and immersed in the same fixative for 2 hr at 4°C. After washing thoroughly with 0.1 M PB containing 7.5% sucrose, tissue blocks were dehydrated in graded ethanol and embedded in epoxy resin (Epon 812; TAAB #T026; purchased from Nissin EM Co. Ltd., Tokyo, Japan). Serial sections of 0.5- μ m thickness were cut from the tissue blocks with an ultramicrotome and mounted on microscopic slides.

After removal of the resin by sodium methoxide (Grube and Kusumoto 1986), semi-thin sections were treated with 0.05% citraconic anhydride solution (Immunosaver; Nissin EM Co. Ltd.) for 20 min at 60°C as an antigen retrieval procedure (Namimatsu et al. 2005), and then incubated with 2% normal donkey serum (30 min, 20°C) for blocking. After these pretreatments, tissue sections were incubated with a mixture of primary antibodies of different species (rabbit-, mouse-, sheep- or goat-origin) for 18 hr at 4°C. The sections were subsequently incubated with a mixture of appropriate sets of Alexa Fluor 350-, 488-, 594-labeled secondary antibodies for 1 hr at 20°C. Then coverslips were mounted on the tissue sections in 90% glycerol (v/v in PBS) containing 0.1% p-phenylenediamine dihydrochloride (Sigma-Aldrich). Between each step, the sections were washed three times in 0.01 M PB (pH 7.4) containing 0.5 M NaCl and 0.1% Tween 20. Stained sections were viewed with an epifluorescence microscope (Olympus, Tokyo, Japan).

For observations by laser confocal microscopy, cryosections of the pituitary tissues were prepared after fixation by perfusion and cryoprotection. Briefly, pieces of fixed pituitary tissue described above were rinsed with 0.1 M PB containing 7.5% sucrose and were immersed sequentially in 15% sucrose (for 6 hr) and 30% sucrose (for 12 hr) solutions buffered in 0.1 M PB (pH 7.4) at 4°C; then the tissue blocks were frozen at -30°C in the

Tissue-Tek O.C.T. compound (Sakura Finetek, Tokyo, Japan). Tissue sections of 15- μ m thickness were cut from the frozen tissue blocks with a cryostat (Leica Microsystems GmbH, Wetzlar, Germany) and mounted on microscopic slides. After these sections were treated with 0.05% citraconic anhydride solution (Immunosaver, Nissin EM Co. Ltd.) for 20 min, 60°C, and subsequently with 2% normal donkey serum (30 min, 20°C) for blocking. Sections were incubated with a mixture of primary antibodies of different species (rabbit-, mouse-, sheep- or goat-origin) for 18 hr at 4°C. The sections were then incubated with a mixture of appropriate sets of Alexa Fluor 488-labeled, 594-labeled, and biotinylated secondary antibodies for 1 hr at 20°C and were further incubated with Alexa Fluor 405-conjugated streptavidin for 1 hr at 20°C. Between each step, the sections on microscopic slides were washed three times in 0.01 M PB (pH 7.4) containing 0.5 M NaCl and 0.1% Tween 20. After coverslips were mounted similarly as described above, stained sections were viewed with a laser confocal microscope (FV-1000D, Olympus).

Scanning electron microscopy

Tissue preparation for scanning electron microscopy was described previously (Tanaka and Mitsushima 1984; Koga and Ushiki 2006). Briefly, anesthetized male rats (n=5) at 8 weeks of age were perfused with physiological saline followed by a mixture of 0.5% glutaraldehyde (GA)—0.5% PFA in 0.1 M PB (pH 7.4). After fixation by perfusion, pituitaries were cut into small pieces and directly immersed in 1% Osmium tetroxide (OsO₄) in 0.1 M PB (pH 7.4) for 2 hr at 4°C. Then the tissue blocks were washed thoroughly with 0.1 M PB, immersed in 25% and 50% dimethyl sulfoxide (DMSO) for 30 min each, and then frozen on a metal plate that had been deeply chilled with liquid nitrogen. The frozen tissue blocks were cracked into two pieces with a screwdriver and a hammer and immediately transferred into 50% DMSO for thawing. After the freeze-cracked pituitary tissue blocks were rinsed in 0.1 M PB for 1 hr at

4°C, they were placed in 0.1% OsO₄ diluted with 0.1 M PB (pH 7.4) for 72 hr at 20°C–22°C under fluorescent light illumination. During maceration of the pituitary tissues, the 0.1% OsO₄ solution was renewed every 24 hr. The macerated specimens were further fixed in 1% OsO₄ in 0.1 M PB (pH 7.4) for 1 hr, washed in 0.1 M PB for 1 hr, and conductive stained by treating with 1% tannic acid in 0.1 M PB (2 hr, 20°C) and 1% OsO₄ in 0.1 M PB (1 hr, 20°C). After conductive staining, the samples were dehydrated in graded ethanol, transferred into isoamyl acetate, and dried in a critical point dryer (HCP-2, Hitachi Koki Co. Ltd., Tokyo, Japan) using liquid CO₂. The dried samples were mounted onto a metal plate and coated with platinum-palladium in an ion-sputter coater (E1010, Hitachi Koki Co. Ltd.), and then were observed with an in-lens type scanning electron microscope (S-5000, Hitachi High Technologies, Tokyo, Japan).

Immunoelectron microscopy

Rats (n=5) at 8 weeks of age were anesthetized with ketamine/xylazine as described above and then perfused with physiological saline followed by 100 ml of 2% GA–2% PFA in 0.1 M PB (pH 7.4). After fixation by perfusion, pituitaries were cut into small pieces and immersed in the same fixative for 2 hr at 4°C. After washing thoroughly with 0.1 M PB containing 7.5% sucrose, tissue blocks were further fixed with 1% OsO₄ in 0.1 M PB containing 7.5% sucrose for 1 hr at 4°C. The tissue blocks were then washed thoroughly with 0.1 M PB containing 7.5% sucrose, dehydrated in graded ethanol, and embedded in epoxy resin (Epon 812). After ultra-thin sections from the tissue blocks embedded in Epon 812 were etched with 1% sodium methoxide for 30 sec prior to the immunostaining procedures, they were incubated with 5% non-immune goat serum for blocking (20 min, 20°C). Sections were further incubated with an anti- LHβ (rabbit polyclonal, diluted 1:100) antiserum for 12 hr at 4°C and then treated with colloidal gold-conjugated goat anti-rabbit IgG for 1 hr at 20°C (size of gold particles: 10 nm

in diameter). Between each step, the sections on grids were washed three times in 0.02 M Tris-HCl buffered 0.5 M saline, pH 8.2, containing 0.1% BSA.

Alternatively, similarly anesthetized rats (n=5) at 8 weeks of age were perfused with physiological saline, followed by 100 ml of 0.5% GA–0.5% PFA in 0.1 M PB (pH 7.4). Immediately after fixation by perfusion, pituitaries were cut into small pieces and directly immersed in 0.5% OsO₄ in 0.1 M PB for 1 hr at 4°C. Then the tissue blocks were washed thoroughly with 0.1 M PB containing 7.5% sucrose, dehydrated in 70% ethanol containing 1% phosphotungstic acid (Wako Pure Chemical, Osaka, Japan) three times for 20 min at 4°C, and then infiltrated into pure LR White resin (London Resin Co., Hampshire, UK) monomer. The resin solution was changed three times during infiltration (20 min each at 4°C), and finally the tissue blocks were placed at the bottom of gelatin capsules filled with fresh LR White resin and polymerized for 24 hr at 60°C.

Immunogold labeling of pituitary tissues embedded in LR White resin was performed as described previously (Sakai et al. 2005; Hosaka et al. 2007). For removal of OsO₄, ultra-thin sections from the LR white-embedded tissues were treated in 1% sodium metaperiodate (Wako Pure Chemical) for 10 min at 20°C prior to the immunogold labeling. Then the sections were incubated with 5% normal goat serum for blocking (20 min, 20°C) and further incubated with the primary antibodies for 12 hr at 4°C as follows: anti-LHβ (rabbit polyclonal, diluted 1:5000); anti-GM130 (rabbit polyclonal, 1:10); anti-TGN38 (mouse monoclonal, 1:10); anti-α-tubulin (1:50); and anti-γ-tubulin (1:50). For double immunostaining, the two-face technique of Bendayan (1982) was applied. Intracellular localization of two distinct antigens was distinguished by labeling with different sizes of colloidal gold particles (size of particles: 5, 10, and 15 nm in diameter) conjugated to appropriate secondary antibodies. Between each step, the sections on grids were washed three times in 0.02 M Tris-HCl buffered 0.5 M saline, pH 8.2, containing 0.1% BSA. Following

the immunoreactions, the sections were contrasted with saturated aqueous solutions of uranyl acetate and lead citrate and examined with an electron microscope (JEM-1010, JEOL, Tokyo, Japan).

Results

Overall Shape and Ultrastructure of the Golgi Apparatus in Pituitary Gonadotropes

As previously reported (Koga and Ushiki 2006), well-developed Golgi apparatus in a ball-like shape was occasionally observed in the rat anterior pituitary gland by scanning electron microscopy (Fig. 1). Stacks of fenestrated cisternae spherically enveloped a part of cytoplasm near to the cell nucleus, and there were relatively large openings on the wall of the ball-shaped Golgi apparatus (Fig. 1A; arrowheads). Secretory granules/vesicles and tubular extensions derived from the Golgi and RER cisternae were frequently observed inside of the large openings, suggesting that the large openings penetrating the entire Golgi stacks likely provide trafficking routes for the tubulovesicles/granules between two segregated cytoplasmic spaces, inside and outside of the Golgi sphere.

To identify immunocytochemically the cell type containing spherical Golgi apparatus, we examined the colocalization of representative marker molecules for the Golgi apparatus and pituitary hormones on serial semi-thin sections of anterior pituitary tissue. After immunocytochemical staining for GM130, spheroidal Golgi apparatus could be traced as circular profiles on a series of consecutive semi-thin sections (Fig. 2). By double/triple immunostaining of these serial sections simultaneously with antibodies against pituitary hormones, the cells containing the spherical Golgi apparatus were identified as gonadotropes (Fig. 2; white arrowheads).

Observations with a transmission electron microscope were consistent with the findings described above; typical pituitary gonadotropes immunolabeled with an anti-LH antiserum contained well-developed stacks of Golgi apparatus, of which profiles were circularly arranged (Fig. 3). The circular arrangement of the Golgi stacks did not completely enclose the inner cytoplasm from the outside of the Golgi sphere, but rather both inner and outer cytoplasmic spaces were interconnected through gaps in the circular wall of the Golgi

cisternae. In the inner area of the Golgi apparatus, immature secretory granules and centrioles were frequently observed (Fig. 3A; arrows and white arrowheads, respectively). From the central area of the Golgi apparatus in the cell, radiating microtubules extended to the cell periphery, passing through the gaps in the circular arrangement of the Golgi stacks (Fig. 3B, C, black arrowheads).

Polarity of the Golgi Apparatus in Gonadotropes

Frequent occurrence of immature secretory granules inside spherical Golgi apparatus suggested that the inner side of the Golgi stacks is the trans face. To confirm the precise polarity of the Golgi apparatus, the immunocytochemical localization of GM130 and TGN38 was examined at the electron microscopic level.

As shown in Fig. 4, immunogold particles indicative of GM130 were localized to the outer surface of the spherical Golgi apparatus, whereas those indicative of TGN38 were localized to the inner surface. These immunocytochemical findings clearly indicate that the outer surface of the Golgi sphere functions as the cis compartment that receives precursors of secretory products from the RER, whereas the inner side of the sphere is the trans compartment, from which immature secretory granules and primary lysosomes are newly generated.

The intracellular distribution of Binding immunoglobulin protein (BiP) and γ -adaptin confirmed the findings described above; BiP immunoreactivity, indicative of RER distribution, was predominantly localized outside of the Golgi apparatus in the gonadotropes, whereas the intense immunocytochemical signal for γ -adaptin, which indicates the localization of AP1/clathrin-coated vesicles, was confined to the interior (Fig. 5).

Organization of the Microtubule Network within Gonadotropes

Since microtubules were frequently observed in the central area of spheroidal Golgi apparatus in the pituitary gonadotropes, the distribution of tubulins was immunocytochemically examined.

By immunofluorescence microscopy, α -tubulin was principally observed to accumulate in the inner area of the Golgi apparatus and was especially concentrated on a hub-like spot at the center of the circular profile (Fig. 6A, arrows). In addition to the inner area, the microtubule networks were also distributed densely around the outer surface. Outside of these, arrays of radiating microtubules extending to the cell periphery were sparsely distributed.

To demonstrate the distribution of relatively stable bundles of microtubules, the intracellular localization of acetylated α -tubulin was immunocytochemically visualized in a gonadotrope (Fig. 6B, C). At an equatorial plane of the spherical Golgi apparatus in the gonadotrope, microtubule bundles immunolabeled with an anti-acetylated α -tubulin antibody penetrated the circular profile of the Golgi apparatus (Fig. 6B, arrow) and extended radially to the periphery of the cell (Fig. 6B, arrowheads). At the outer surface of the Golgi sphere, the bundles of microtubules partially diverged from the radiating ones, bending along the outer surface of the Golgi apparatus. In a view of a tangential plane at the pole of the Golgi sphere, bundles of relatively stable microtubules appeared to form a meshwork covering the outer surface of the spherical Golgi apparatus (Fig. 6C). In this surface view at the polar plane, openings on the spherical Golgi wall were clearly discerned, through which thick bundles of microtubules penetrated (Fig. 6C, arrow).

The location of the microtubule organizing center (MTOC) was also examined by labeling the pituitary gonadotrope immunocytochemically with an anti- γ -tubulin antibody (Fig. 7A). A three-dimensional image reconstructed with a laser confocal microscope confirmed the spherical shape of the Golgi apparatus in pituitary gonadotropes. A spot

labeled intensely with anti- γ -tubulin antibody was localized inside of the Golgi apparatus in gonadotropes (Fig. 7A, arrows). In addition, γ -tubulin was found to accumulate circumferentially on the outer surface, similarly to α -tubulin.

By immunogold labeling at the electron microscopic level, the distribution of the microtubules was confirmed; microtubule tracks linearly labeled with an anti- α -tubulin antibody were frequently observed (Fig. 7B). γ -Tubulin was specifically localized around the centrioles in the central area of the circular Golgi profile (Fig. 7C), suggesting that the centrioles and associated materials function as an MTOC, from which the radiating microtubules are likely to have originated.

Discussion

Previous observations mainly based on polarized epithelial and exocrine cells have provided a widely shared image of the Golgi apparatus as cup-shaped or hemispherical, of which the convex and concave faces confront the RER and plasma membrane, respectively (Farquhar and Palade 1981, 1998). The present immunocytochemical study, however, demonstrated that pituitary gonadotropes contain spherical Golgi apparatus, of which the trans face (the exit side) is not the outer but the inner surface of the sphere. The MTOC is situated at the center of the spherical Golgi apparatus, from which radiating microtubules isotropically extended to the cell periphery through gaps in the wall of the Golgi stack.

The spatial configuration of the Golgi apparatus is closely related to the overall cellular polarity, especially the arrangement and orientation of microtubules (Thyberg and Moskalewski 1999; Allan et al. 2002; Murshid and Presley 2004; Sütterlin and Colanzi 2010). In typical polarized epithelial cells, the minus and plus ends of microtubule bundles principally direct to the apical and basolateral membrane domains, respectively (Meads and Schroer 1995; Müsch 2004). The coherent and directional array of the microtubules along the longitudinal axis of polarized epithelial cells can facilitate differential transport of tubulovesicular carriers conveying molecules specific to the apical and basolateral membrane domains, resulting in the establishment of these two distinct domains on the cell surface (Drubin and Nelson 1996; Müsch 2004). The cup-like shape of the Golgi apparatus observed in the polarized exocrine cells possibly corresponds to the distinctive cellular polarity of the cell; the maturing face of the Golgi apparatus should closely confront a restricted area of the cell surface designated as apical domain, from which a large amount of secretory materials are exocytosed specifically to the luminal space of the acinus.

In contrast to polarized exocrine cells, the secretion site for exocytosis of endocrine cells is less strictly confined to specialized subdomain(s) on the cell surface. The arrangement

of the microtubules within endocrine cells is also very symmetrical; microtubules radiate to the cell periphery from a single MTOC at the center of the cell, as we demonstrated above in pituitary gonadotropes. The spheroidal shape of the Golgi apparatus within gonadotropes possibly reflects the poor polarity in the cell surface and the highly symmetrical arrangement of microtubule arrays. As far as we observed, pituitary somatotropes and melanotrophs also possessed ball-shaped Golgi apparatus, although the size of the Golgi sphere of these cells appeared to be smaller than that of gonadotropes (data not shown). The Golgi apparatus of thyrotropes also exhibited a spherical configuration but likely contained larger amount of non-compact regions than that of gonadotropes. In contrast, the Golgi apparatus of mammatropes and corticotropes were considerably distorted. Nevertheless, the cisternae of these cells were not simply composed of an open ribbon-like structure but rather enclosed a certain amount of cytoplasm of the post-Golgi compartment as a three-dimensionally organized wall or network, consistent with previous findings from stereoscopic observation of rat mammatropes (Rambourg et al. 1992). Since some endocrine cells putatively secrete their secretory products preferentially to certain specialized domains on the cell surface near blood vessels, the possible asymmetry in the intracellular arrangement of microtubule arrays results in diversity of the overall shape of the Golgi apparatus observed in the pituitary gland. The detailed characteristics in the ultrastructure and spatial configuration of the Golgi apparatus observed in various endocrine cells of the pituitary gland will be independently described elsewhere.

Besides endocrine cells, mesenchyme-derived cells such as fibroblasts are regarded as non-polarized cells, although the three-dimensional symmetry of their Golgi apparatus has not been reported to date. The high motility as well as the potential proliferative property of these cells may reduce the symmetry of the overall configuration of the Golgi apparatus; incessant remodeling of the intracellular microtubule architecture possibly distorts the

theoretical symmetry in the global configuration of their Golgi apparatus (Small et al. 2002; Siegrist and Doe 2007; Vinogradova et al. 2009). Overall peptide-producing endocrine cells such as gonadotropes could be more suitable as a model of poorly polarized cells instead of fibroblasts for analyzing the relationship between cell polarity and the configuration of the Golgi apparatus.

In addition to the overall configuration discussed above, the peculiar polarity of the Golgi apparatus within gonadotropes could be explained according to the intracellular arrangement and orientation of microtubules, since the positioning and orientation of the Golgi apparatus are putatively determined by the balance of the antero- and retrograde transport of the tubulovesicular carriers along microtubules in the pre- and post-Golgi compartments (Cole and Lippincott-Schwartz 1995; Lippincott-Schwartz 1998).

Intracellular transporting carriers, such as secretory granules/tubulovesicles and endosomes, use the motor proteins in context (Goodson et al. 1997; Hehnlly and Stamnes 2007; Brownhill et al. 2009). In the pre-Golgi compartment, coat protein II (COPII)-coated vesicles use dynein for anterograde trafficking from the RER to the cis side of Golgi (Presley et al. 1997; Harada et al. 1998; Watson et al. 2005), whereas coat protein I (COPI)-coated tubulovesicles use kinesin/KIFs for retrograde trafficking from the Golgi to the RER (Lippincott-Schwartz et al. 1995; Dorner et al. 1998; Stauber et al. 2006). In the post-Golgi compartment, secretory granules/tubulovesicles and newly generated primary lysosomes are likely transported by kinesin/Kinesin superfamily proteins (KIFs) for anterograde trafficking from the trans side of the Golgi (Kreitzer et al. 2000; Nakagawa et al. 2000; Varadi et al. 2002; Jaulin et al. 2007), whereas endocytosed tubulovesicles are likely transported by dyneins for retrograde trafficking from the plasma membrane to the cell central around the trans-Golgi compartment (Blocker et al. 1997).

The isotropically radiating arrays of microtubules originated from the center of spherical Golgi apparatus possibly streamline the trafficking process of the wide variety of granular/tubulovesicular carriers described above within the pituitary gonadotrope (Fig. 8). Minus-end-directed motors, such as dyneins (Vallee et al. 2004), mediate the centripetal movements of the carriers, COPII-coated vesicles and endocytosed tubulovesicles in the pre- and post-Golgi compartments, respectively. In contrast, plus-end-oriented motors, like kinesins and most of KIFs (Hirokawa and Noda 2008), mediate the centrifugal movements of the carriers, COPI-coated vesicles and secretory granules/tubulovesicles in the pre- and post-Golgi compartments, respectively. All of the movements of the transporting tubulovesicular carriers and granules along microtubules in pituitary gonadotropes could be explained by the findings described above.

In addition to the isotropically radiating arrays from the central MTOC, relatively dense accumulation of α - and γ -tubulin was observed around the outer surface of the spherical Golgi apparatus in gonadotropes by confocal laser scanning microscopy. At least to some extent, the tubulins accumulated on the cis side of the Golgi apparatus form a meshwork of relatively stable microtubule bundles, as demonstrated in the present study. The tangential meshwork of the microtubules covering the outer surface of the Golgi apparatus possibly plays a role in clustering Golgi mini-stacks into a compact spherical organelle. As another possibility, tubulins could form short and labile tracks between the cis face of the Golgi apparatus and the RER distributed in the outside of the Golgi. Recent studies demonstrating that certain Golgi-related proteins are specifically associated with γ -tubulin (Chabin-Brion et al. 2001; Rios et al. 2004; Efimov et al. 2007; Rivero et al. 2009) suggest that the outer surface of spheroidal Golgi in gonadotropes efficiently acts as the origin of such short microtubule tracks (Rios and Bornens 2003; Lüders and Stearns 2007; Sütterlin and Colanzi 2010). These short tracks putatively contribute to both antero- and retrograde

tubulovesicular transport of a large amount of gonadotropins and other secretory proteins for their quality control processes in the pre-Golgi compartment.

In summary, our present study demonstrated the overall configuration of the Golgi apparatus within pituitary gonadotropes, which strongly reflects the characteristics in the cellular organization of the poorly polarized endocrine cells. Although isolated cultured cells have been mainly used for the investigations of the dynamics of the Golgi apparatus so far, its highly symmetric and isotropic architecture in pituitary gonadotropes possibly provides an alternative good experimental model to analyze this issue. Since the functional state of pituitary gonadotropes can be specifically modulated with endocrinological methods, further analyses of these cells under experimentally stimulated/suppressed conditions would provide more insight into the relationship between the organization and function of the Golgi apparatus.

Acknowledgments

This work was supported in part by a Grant-in-Aid for Scientific Research (C) from the Japan Society for the Promotion of Science (JSPS) (#22590185) and a research grant from the Suhara Memorial Foundation.

Literature Cited

Allan VJ, Thompson HM, McNiven MA (2002) Motoring around the Golgi. *Nat Cell Biol* 4:E236-242

Bendayan M (1982) Double immunocytochemical labeling applying the protein A-gold technique. *J Histochem Cytochem* 30:81-85

Blocker A, Severin FF, Burkhardt JK, Bingham JB, Yu H, Olivo JC, Schroer TA, Hyman AA, Griffiths G (1997) Molecular requirements for bi-directional movement of phagosomes along microtubules. *J Cell Biol* 137:113-129

Brownhill K, Wood L, Allan V (2009) Molecular motors and the Golgi complex: staying put and moving through. *Semin Cell Dev Biol* 20:784-792

Chabin-Brion K, Marceiller J, Perez F, Settegrana C, Drechou A, Durand G, Pous C (2001) The Golgi complex is a microtubule-organizing organelle. *Mol Biol Cell* 12:2047-2060

Clermont Y, Rambourg A, Hermo L (1995) Trans-Golgi network (TGN) of different cell types: three-dimensional structural characteristics and variability. *Anat Rec* 242:289-301

Cole NB, Lippincott-Schwartz J (1995) Organization of organelles and membrane traffic by microtubules. *Curr Opin Cell Biol* 7:55-64

De Matteis MA, Luini A (2008) Exiting the Golgi complex. *Nat Rev Mol Cell Biol* 9:273-284

Dorner C, Ciossek T, Muller S, Moller PH, Ullrich A, Lammers R (1998) Characterization of KIF1C, a new kinesin-like protein involved in vesicle transport from the Golgi apparatus to the endoplasmic reticulum. *J Biol Chem* 273:20267-20275

Drubin DG, Nelson WJ (1996) Origins of cell polarity. *Cell* 84:335-344

Efimov A, Kharitonov A, Efimova N, Loncarek J, Miller PM, Andreyeva N, Gleeson P,

- Galjart N, Maia AR, McLeod IX, Yates JR, 3rd, Maiato H, Khodjakov A, Akhmanova A, Kaverina I (2007) Asymmetric CLASP-dependent nucleation of noncentrosomal microtubules at the trans-Golgi network. *Dev Cell* 12:917-930
- Farquhar MG, Palade GE (1981) The Golgi Apparatus (Complex)-(1954-1981)-from artifact to center stage. *J Cell Biol* 91:77s-103s
- Farquhar MG, Palade GE (1998) The Golgi apparatus: 100 years of progress and controversy. *Trends Cell Biol* 8:2-10
- Goodson HV, Valetti C, Kreis TE (1997) Motors and membrane traffic. *Curr Opin Cell Biol* 9:18-28
- Griffiths G, Simons K (1986) The trans Golgi network: sorting at the exit site of the Golgi complex. *Science* 234:438-443
- Grube D, Kusumoto Y (1986) Serial semithin sections in immunohistochemistry: techniques and applications. *Arch Histol Jpn* 49:391-410
- Harada A, Takei Y, Kanai Y, Tanaka Y, Nonaka S, Hirokawa N (1998) Golgi vesiculation and lysosome dispersion in cells lacking cytoplasmic dynein. *J Cell Biol* 141:51-59
- Hehnly H, Stamnes M (2007) Regulating cytoskeleton-based vesicle motility. *FEBS Lett* 581:2112-2118
- Hirokawa N, Noda Y (2008) Intracellular transport and kinesin superfamily proteins, KIFs: structure, function, and dynamics. *Physiol Rev* 88:1089-1118
- Hosaka M, Watanabe T, Yamauchi Y, Sakai Y, Suda M, Mizutani S, Takeuchi T, Isobe T, Izumi T (2007) A subset of p23 localized on secretory granules in pancreatic beta-cells. *J Histochem Cytochem* 55:235-245
- Jaulin F, Xue X, Rodriguez-Boulan E, Kreitzer G (2007) Polarization-dependent selective transport to the apical membrane by KIF5B in MDCK cells. *Dev Cell* 13:511-522
- Koga D, Ushiki T (2006) Three-dimensional ultrastructure of the Golgi apparatus in different

- cells: high-resolution scanning electron microscopy of osmium-macerated tissues. *Arch Histol Cytol* 69:357-374
- Kreitzer G, Marmorstein A, Okamoto P, Vallee R, Rodriguez-Boulan E (2000) Kinesin and dynamin are required for post-Golgi transport of a plasma-membrane protein. *Nat Cell Biol* 2:125-127
- Lippincott-Schwartz J (1998) Cytoskeletal proteins and Golgi dynamics. *Curr Opin Cell Biol* 10:52-59
- Lippincott-Schwartz J, Cole NB, Marotta A, Conrad PA, Bloom GS (1995) Kinesin is the motor for microtubule-mediated Golgi-to-ER membrane traffic. *J Cell Biol* 128:293-306
- Lüders J, Stearns T (2007) Microtubule-organizing centres: a re-evaluation. *Nat Rev Mol Cell Biol* 8:161-167
- Marsh BJ (2005) Lessons from tomographic studies of the mammalian Golgi. *Biochim Biophys Acta* 1744:273-292
- Meads T, Schroer TA (1995) Polarity and nucleation of microtubules in polarized epithelial cells. *Cell Motil Cytoskeleton* 32:273-288
- Mellman I, Simons K (1992) The Golgi complex: in vitro veritas? *Cell* 68:829-840
- Mogelsvang S, Marsh BJ, Ladinsky MS, Howell KE (2004) Predicting function from structure: 3D structure studies of the mammalian Golgi complex. *Traffic* 5:338-345
- Murshid A, Presley JF (2004) ER-to-Golgi transport and cytoskeletal interactions in animal cells. *Cell Mol Life Sci* 61:133-145
- Müsch A (2004) Microtubule organization and function in epithelial cells. *Traffic* 5:1-9
- Nakagawa T, Setou M, Seog D, Ogasawara K, Dohmae N, Takio K, Hirokawa N (2000) A novel motor, KIF13A, transports mannose-6-phosphate receptor to plasma membrane through direct interaction with AP-1 complex. *Cell* 103:569-581

- Namimatsu S, Ghazizadeh M, Sugisaki Y (2005) Reversing the effects of formalin fixation with citraconic anhydride and heat: a universal antigen retrieval method. *J Histochem Cytochem* 53:3-11
- Presley JF, Cole NB, Schroer TA, Hirschberg K, Zaal KJ, Lippincott-Schwartz J (1997) ER-to-Golgi transport visualized in living cells. *Nature* 389:81-85
- Rambourg A, Clermont Y (1990) Three-dimensional electron microscopy: structure of the Golgi apparatus. *Eur J Cell Biol* 51:189-200
- Rambourg A, Clermont Y (1997) Three-dimensional structure of the Golgi apparatus in mammalian cells. In Berger EG, Roth J, eds. *The Golgi Apparatus*. Basel, Birkhäuser Verlag, 37-61
- Rambourg A, Clermont Y, Chretien M, Olivier L (1992) Formation of secretory granules in the Golgi apparatus of prolactin cells in the rat pituitary gland: a stereoscopic study. *Anat Rec* 232:169-179
- Rios RM, Bornens M (2003) The Golgi apparatus at the cell centre. *Curr Opin Cell Biol* 15:60-66
- Rios RM, Sanchis A, Tassin AM, Fedriani C, Bornens M (2004) GMAP-210 recruits gamma-tubulin complexes to cis-Golgi membranes and is required for Golgi ribbon formation. *Cell* 118:323-335
- Rivero S, Cardenas J, Bornens M, Rios RM (2009) Microtubule nucleation at the cis-side of the Golgi apparatus requires AKAP450 and GM130. *EMBO J* 28:1016-1028
- Sakai Y, Hosaka M, Hira Y, Harumi T, Ohsawa Y, Wang H, Takeuchi T, Uchiyama Y, Watanabe T (2003) Immunocytochemical localization of secretogranin III in the anterior lobe of male rat pituitary glands. *J Histochem Cytochem* 51:227-238
- Sakai Y, Hosaka M, Hira Y, Watanabe T (2005) Addition of phosphotungstic acid to ethanol for dehydration improves both the ultrastructure and antigenicity of pituitary tissue

- embedded in LR White acrylic resin. *Arch Histol Cytol* 68:337-347
- Siegrist SE, Doe CQ (2007) Microtubule-induced cortical cell polarity. *Genes Dev* 21:483-496
- Small JV, Geiger B, Kaverina I, Bershadsky A (2002) How do microtubules guide migrating cells? *Nat Rev Mol Cell Biol* 3:957-964
- Stauber T, Simpson JC, Pepperkok R, Vernos I (2006) A role for kinesin-2 in COPI-dependent recycling between the ER and the Golgi complex. *Curr Biol* 16:2245-2251
- Sütterlin C, Colanzi A (2010) The Golgi and the centrosome: building a functional partnership. *J Cell Biol* 188:621-628
- Tanaka K, Mitsushima A (1984) A preparation method for observing intracellular structures by scanning electron microscopy. *J Microsc* 133:213-222
- Tanaka K, Mitsushima A, Fukudome H, Kashima Y (1986) Three-dimensional architecture of the Golgi complex observed by high resolution scanning electron microscopy. *J Submicrosc Cytol* 18:1-9
- Tanaka K, Fukudome H (1991) Three-dimensional organization of the Golgi complex observed by scanning electron microscopy. *J Electron Microsc Tech* 17:15-23
- Thyberg J, Moskalewski S (1999) Role of microtubules in the organization of the Golgi complex. *Exp Cell Res* 246:263-279
- Vallee RB, Williams JC, Varma D, Barnhart LE (2004) Dynein: An ancient motor protein involved in multiple modes of transport. *J Neurobiol* 58:189-200
- Varadi A, Ainscow EK, Allan VJ, Rutter GA (2002) Involvement of conventional kinesin in glucose-stimulated secretory granule movements and exocytosis in clonal pancreatic beta-cells. *J Cell Sci* 115:4177-4189
- Vinogradova T, Miller PM, Kaverina I (2009) Microtubule network asymmetry in motile

cells: role of Golgi-derived array. *Cell Cycle* 8:2168-2174

Watson P, Forster R, Palmer KJ, Pepperkok R, Stephens DJ (2005) Coupling of ER exit to microtubules through direct interaction of COPII with dynactin. *Nat Cell Biol* 7:48-55

Figure Legends

Figure 1. Three-dimensional architecture of the ball-shaped Golgi apparatus observed in the anterior pituitary gland of the male rat. Ball-shaped Golgi apparatus were observed in pituitary tissues using a scanning electron microscope after treatment with a diluted OsO_4 solution. Canal-like openings interconnecting the inner and outer cytoplasmic spaces were discernible through the solid wall of the spherical Golgi apparatus (A; arrowheads). A surface view of ball-shaped Golgi apparatus is demonstrated with a stereo pair of scanning electron microscopic images (B). Bars = 1 μm .

Figure 2. Identification of the cell type containing spherical Golgi apparatus. A semi-thin section (0.5 μm) of rat anterior pituitary gland was simultaneously immunostained with mouse monoclonal anti-GM130 (visualized with Alexa Fluor 594; white and red pseudo colors are assigned in A1 and A2, respectively), sheep polyclonal anti-TGN38 (Alexa Fluor 488; green in A2), and rabbit polyclonal anti-LH (Alexa Fluor 350; blue in A2) antibodies. In addition, four adjacent serial semi-thin sections (B–E) were immunostained with mouse monoclonal anti-GM130 antibody (visualized with Alexa Fluor 594; red in B–E) and goat polyclonal anti-LH antibody (Alexa Fluor 350; blue in B–E). Simultaneously, these sections were immunostained with rabbit polyclonal anti-prolactin (PRL; B), anti-GH (C), anti-ACTH (D), and anti-TSH (E) antibodies (Alexa Fluor 488; green in B–E). Throughout the series of semi-thin sections, circular profiles of the Golgi apparatus were continuously observed in gonadotropes (white arrowheads). R = red; G = green; B = blue. Bar = 10 μm .

Figure 3. Ultrastructure of Golgi apparatus in pituitary gonadotropes. A representative gonadotrope identified on an ultra-thin section of the Epon 812-embedded pituitary tissue by immunocytochemical labeling with rabbit polyclonal anti-LH antiserum and an appropriate

secondary antibody conjugated with colloidal gold particles (10 nm in diameter; A). Partial areas indicated in (A) are further photographed at a higher magnification (B, C). In the inner area of the circular arrangement of the Golgi stacks in the gonadotrope, centrioles (white arrowhead) and immature secretory granules (arrows) were frequently observed. From the center of the Golgi apparatus, radiating microtubules extended to the cell periphery (black arrowheads). Bars = 500 nm.

Figure 4. Polarity of Golgi apparatus in pituitary gonadotropes. By double immunolabeling with anti-GM130 (indicated by 15-nm gold particles) and anti-TGN38 (10-nm gold particles) antibodies, the orientation of the Golgi apparatus was determined on pituitary tissue embedded in LR White resin (A). Partial areas indicated in (A) are further photographed at a higher magnification (B, C). A centriole was observed in the central area of the circular Golgi apparatus (arrowhead). Bars = 500 nm.

Figure 5. Distribution of BiP and γ -adaptn within pituitary gonadotropes. Two adjacent semi-thin sections (thickness: 0.5 μ m each) of rat anterior pituitary gland were immunostained with mouse monoclonal anti-BiP (A) and anti- γ -adaptn (B) antibodies and visualized with an Alexa Fluor 488-conjugated secondary antibody (green pseudo color assigned in A1 and B1). These semi-thin sections were simultaneously immunostained with rabbit polyclonal anti-GM130 (Alexa Fluor 594; red in A1 and B1) and goat polyclonal anti-LH (Alexa Fluor 350; blue in A1 and B1) antibodies. Note that the expression of BiP was apparently higher in gonadotropes than in other endocrine cell types and that BiP immunoreactivity was distributed mainly outside the circular profiles of the Golgi apparatus observed in gonadotropes (A3). R = red; G = green; B = blue. Bar = 10 μ m.

Figure 6. Distribution of α -tubulin within pituitary gonadotropes. (A) A thick section of anterior pituitary gland was immunostained simultaneously with mouse monoclonal anti- α -tubulin (labeled with Alexa Fluor 594; red and white in A1 and A2, respectively), sheep polyclonal anti-TGN38 (Alexa Fluor 488; green in A1), and rabbit polyclonal anti-LH β (Alexa Fluor 405; blue in A1) antibodies. The section was viewed with a laser confocal microscope (thickness of the optical section: 2 μ m). Bar =10 μ m. (B, C) A thick section of anterior pituitary gland was immunostained simultaneously with sheep polyclonal anti-TGN38 (Alexa Fluor 488; green [B1 and C1] and white [B2 and C2]), mouse monoclonal anti-acetylated α -tubulin (Ac- α -Tub; labeled with Alexa Fluor 594; red [B1 and C1] and white [B3 and C3]), and rabbit polyclonal anti-LH β (Alexa Fluor 405; blue in B1 and C1) antibodies. The section was viewed with a laser confocal microscope (thickness of the optical section: 0.5 μ m), and two different optical slices at the equatorial (B) and polar (C) positions of the spherical Golgi apparatus indicated by lines in the three-dimensionally reconstructed x-z (upper panel) and y-z (left panels) views are demonstrated. Note that bundles of the relatively stable microtubule immunolabeled with an anti-acetylated α -tubulin antibody penetrate through the openings on the spherical Golgi wall (arrows) and then extend radially to the cell periphery (arrowheads). Note also that the outer surface of the spherical Golgi apparatus is covered with a meshwork of microtubules. Bar =10 μ m.

Figure 7. Localization of the microtubule organizing center (MTOC) in pituitary gonadotropes. (A) A thick section of anterior pituitary gland was immunostained simultaneously with rabbit polyclonal anti- α -tubulin (labeled with Alexa Fluor 594; red), mouse monoclonal anti-TGN38 (Alexa Fluor 488; green), and goat polyclonal anti-LH (Alexa Fluor 405; blue) antibodies. A three-dimensionally reconstructed image is shown in an orthogonal representation. In addition to the x-y view of the datum plane obtained

originally with the laser confocal microscope (main panel), two reconstructed views, y-z and x-z views, are demonstrated in the left and lower smaller panels, respectively. White lines in the reconstructed images indicate the position of the datum plane demonstrated in the main panel. The series of the original data (thickness of each optical section: 1 μm) for three-dimensional reconstruction are shown in the right of the main panel. The z-axial distance of each optically sliced section from the datum plane is indicated in the left-lower corner of the data. Gonadotropes and the MTOCs immunolabeled with anti- γ -tubulin are indicated by white arrowheads and white arrows, respectively. Bars = 10 μm . (B, C)

Ultra-thin sections of LR White resin-embedded pituitary tissue were immunolabeled with anti- α - (B) and γ - (C) tubulin antibodies, respectively (size of colloidal gold particles: 15 nm). Gonadotropes were identified by immunolabeling with an anti-LH antibody (size of gold particles: 5 nm). Note that the radiating microtubules originating from the center often penetrate the openings in the circular wall-like organization of the Golgi stacks (B; indicated by black arrowheads). The centrioles immunolabeled with anti- γ -tubulin are indicated by white arrowheads. G: the Golgi stacks; bars = 500 nm.

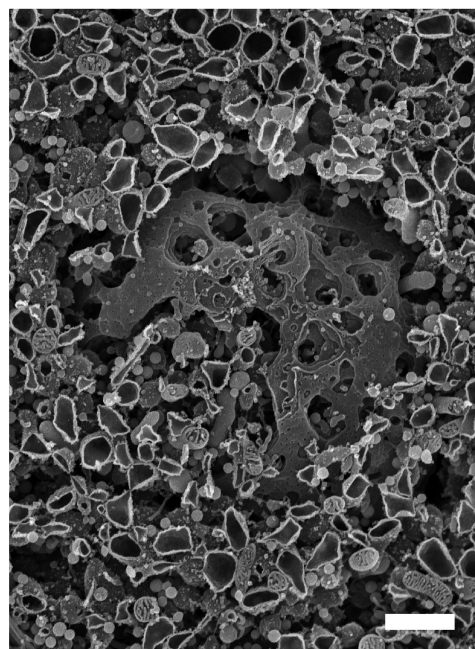
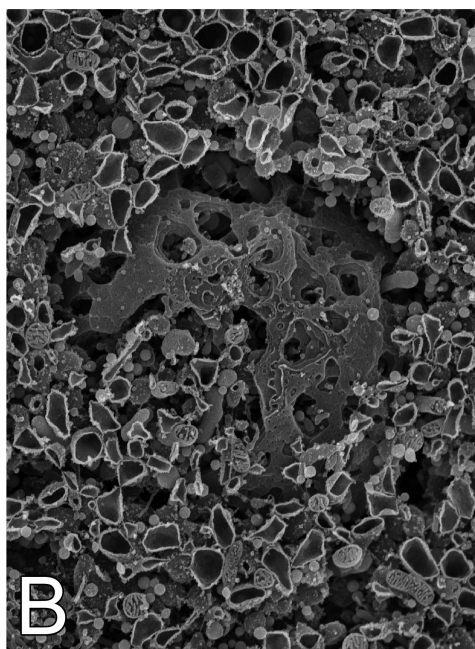
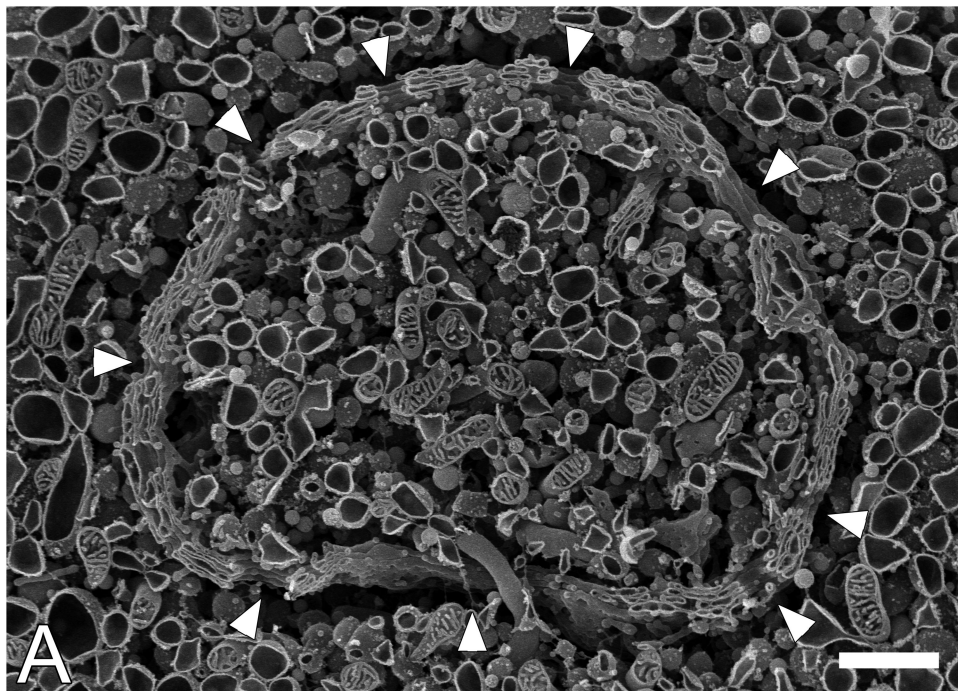
Figure 8. Schematic representation of the architecture of Golgi apparatus and microtubule networks within pituitary gonadotropes.

Supplementary Figure 1. Characterization of the antibodies used in the present study.

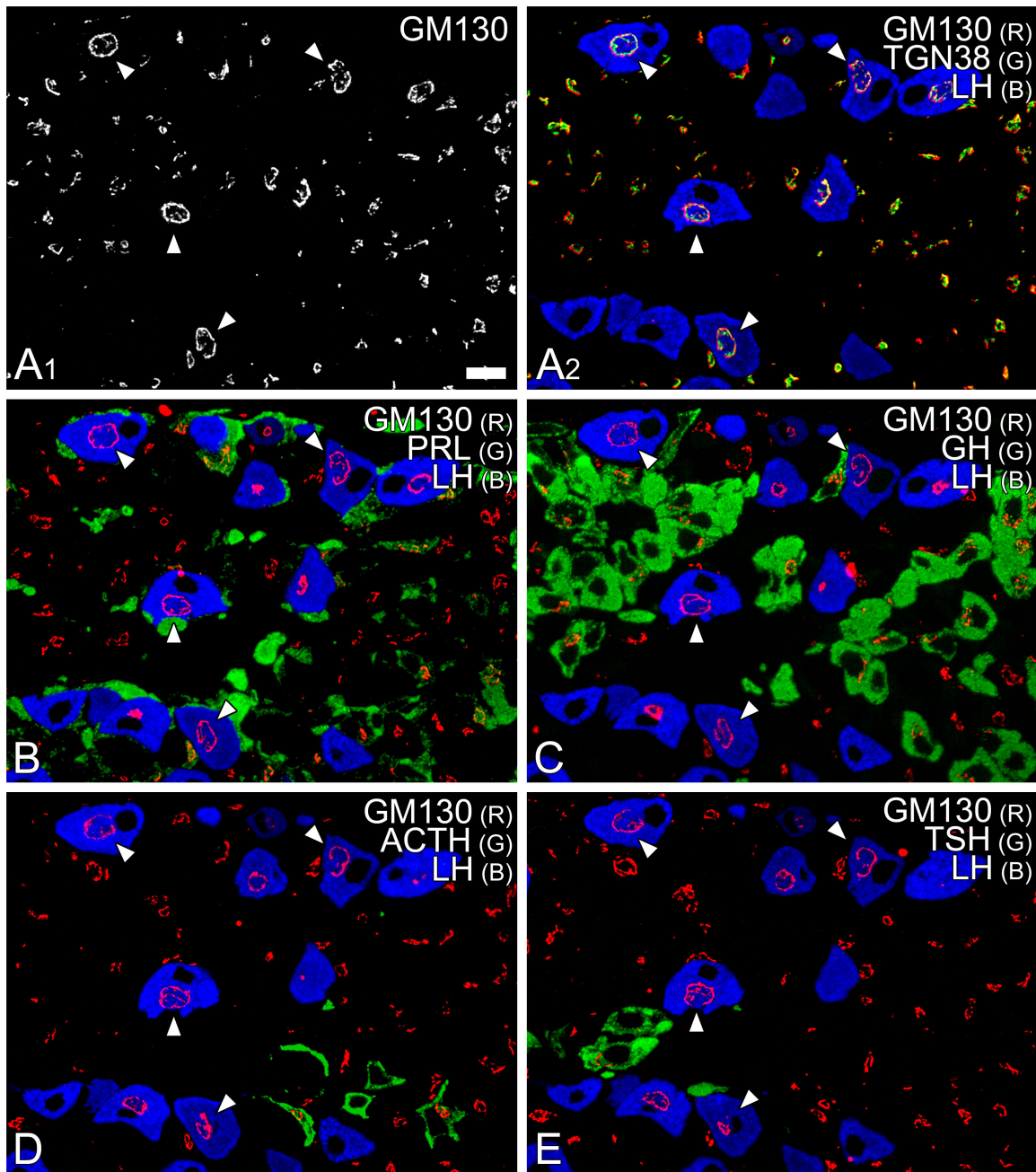
The immunocytochemical findings of the present study were confirmed by using two different sources of antibodies against each antigen, as far as possible. Thick cryosections of the rat pituitary gland were immunostained simultaneously with two different sources of anti-GM130 (A2, A3), anti-TGN38 (B2, B3), anti- α -tubulin (C2, C3), or anti- γ -tubulin (E2, E3) antibodies. The immunostaining patterns of anti-acetylated α -tubulin (mouse

monoclonal; D2) and anti- α -tubulin (rabbit polyclonal; D3) antibodies were also compared. In the left panels, merged images of immunostaining patterns with two different sources of the antibodies (labeled with Alexa Fluor 594 (red) and 488 (green)) and an anti-LH antibody (labeled with Alexa Fluor 405 (blue)) were demonstrated (A1 -E1). Ms: mouse monoclonal antibody, Rb: rabbit polyclonal antibody, Sh: sheep polyclonal antibody. Bar = 10 μ m.

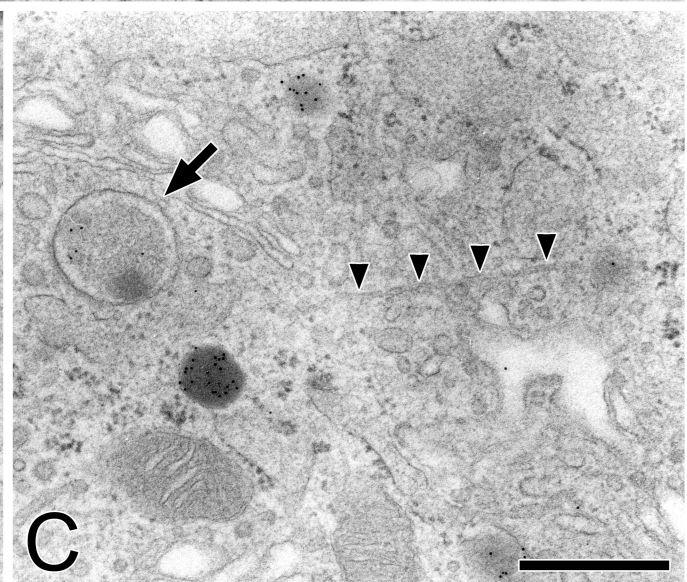
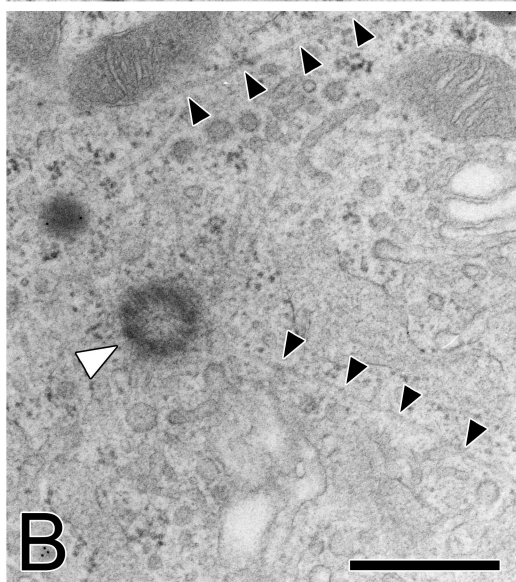
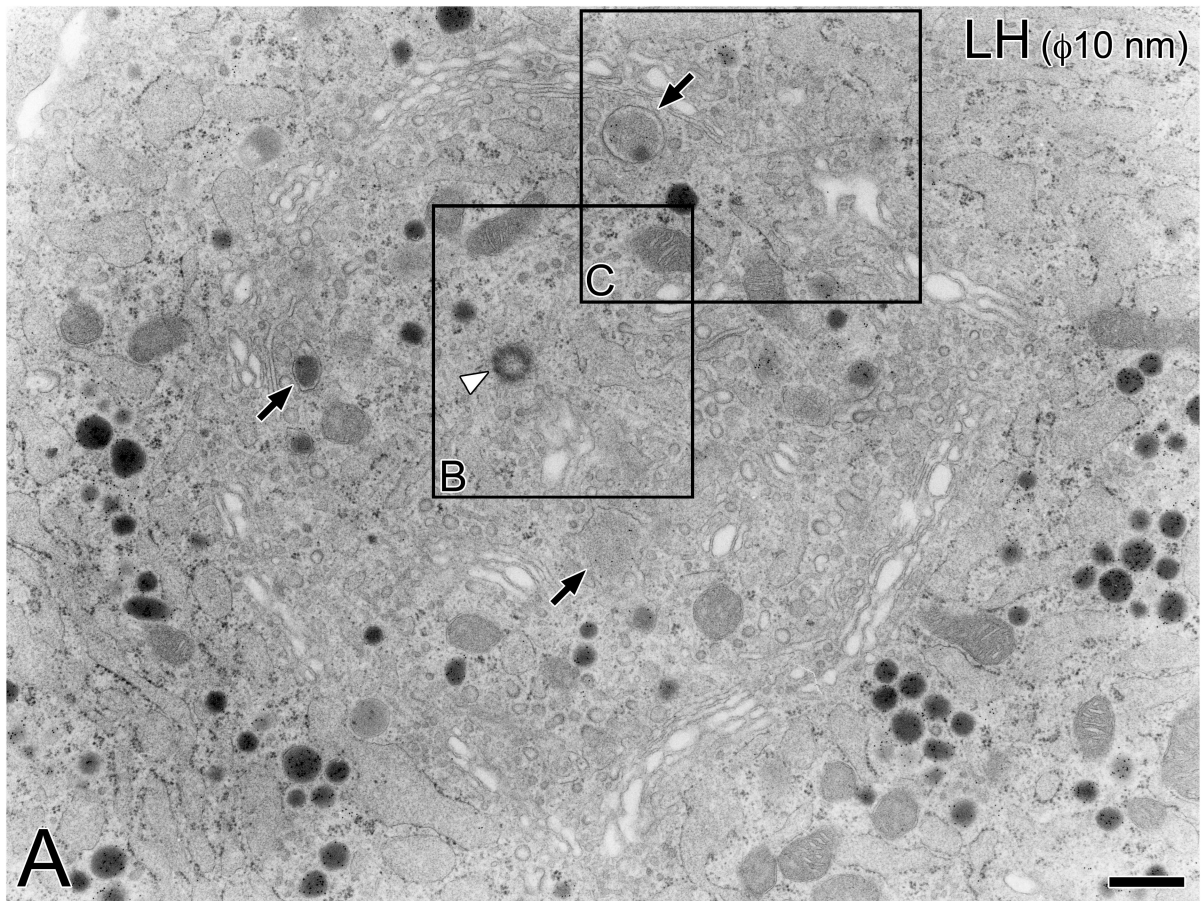
The specificity of these antibodies was also confirmed by immunoblot analyses in extracts of rat representative endocrine tissues including pituitary (Pit), thyroid (Thy) and adrenal (Adr) glands. Ten μ g proteins of each tissue extract were separated onto 12% SDS-PAGE under reducing conditions, transferred to PVDF membranes, and immunostained with the antibodies, as described previously (Sakai et al., 2003). At the right of each immunocytochemical figure panels, blots immunostained with two different sources of anti-GM130 (A4), anti-TGN38 (B4), anti- α -tubulin (C4), and anti- γ -tubulin (E4) antibodies are demonstrated side by side, indicating that these two different sources of antibodies properly recognized identical antigens of appropriate molecular weight (GM130 (130 kDa), TGN38 (85-95 kDa), α -tubulin (55 kDa), and γ -tubulin (48-50 kDa)).



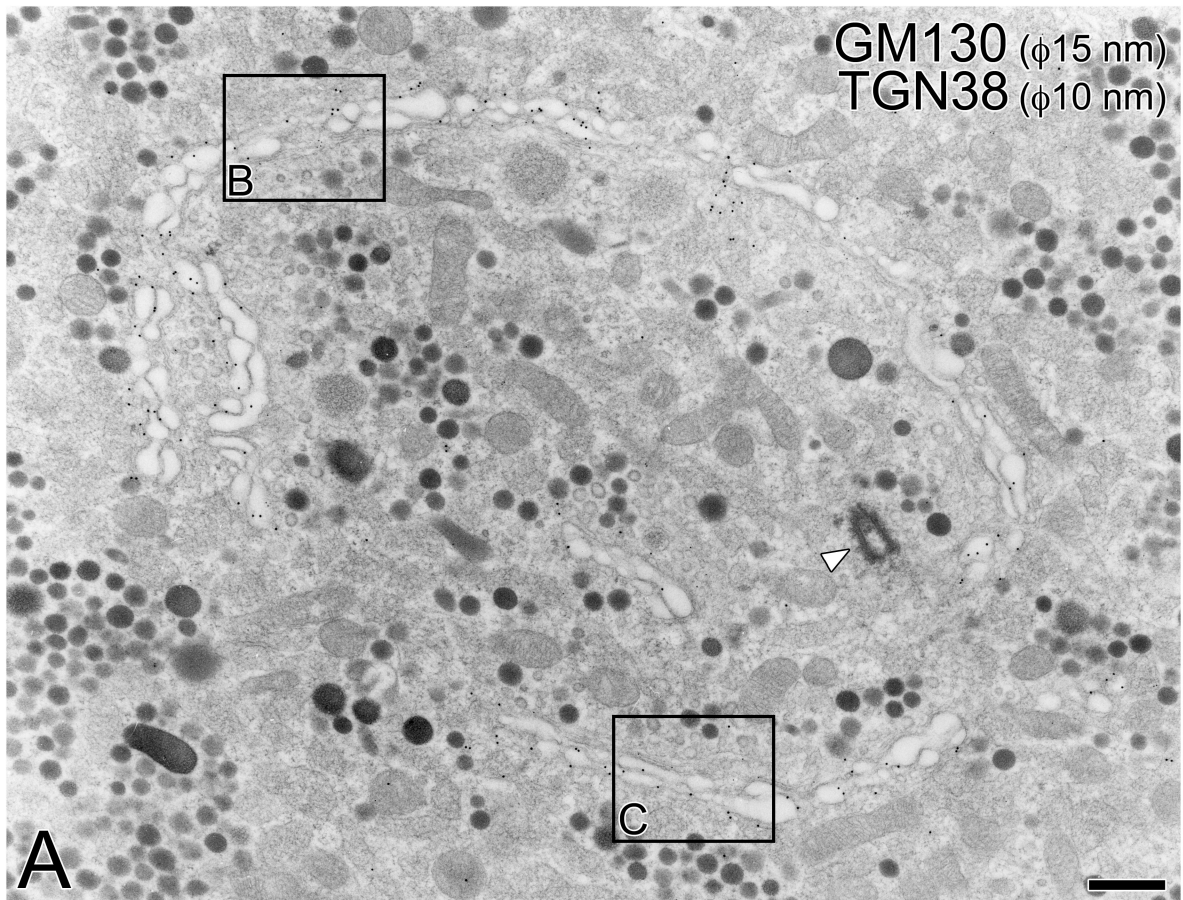
Watanabe et al., Fig. 1



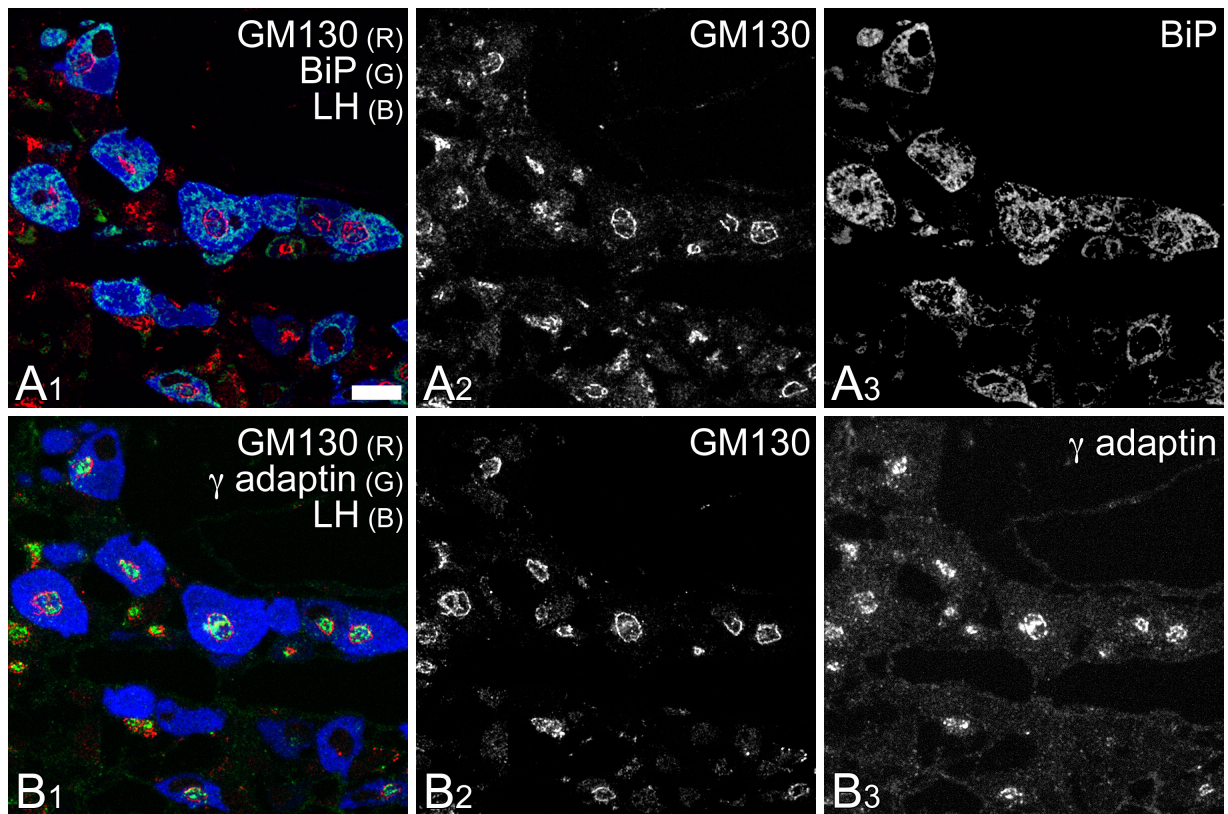
Watanabe et al., Fig. 2



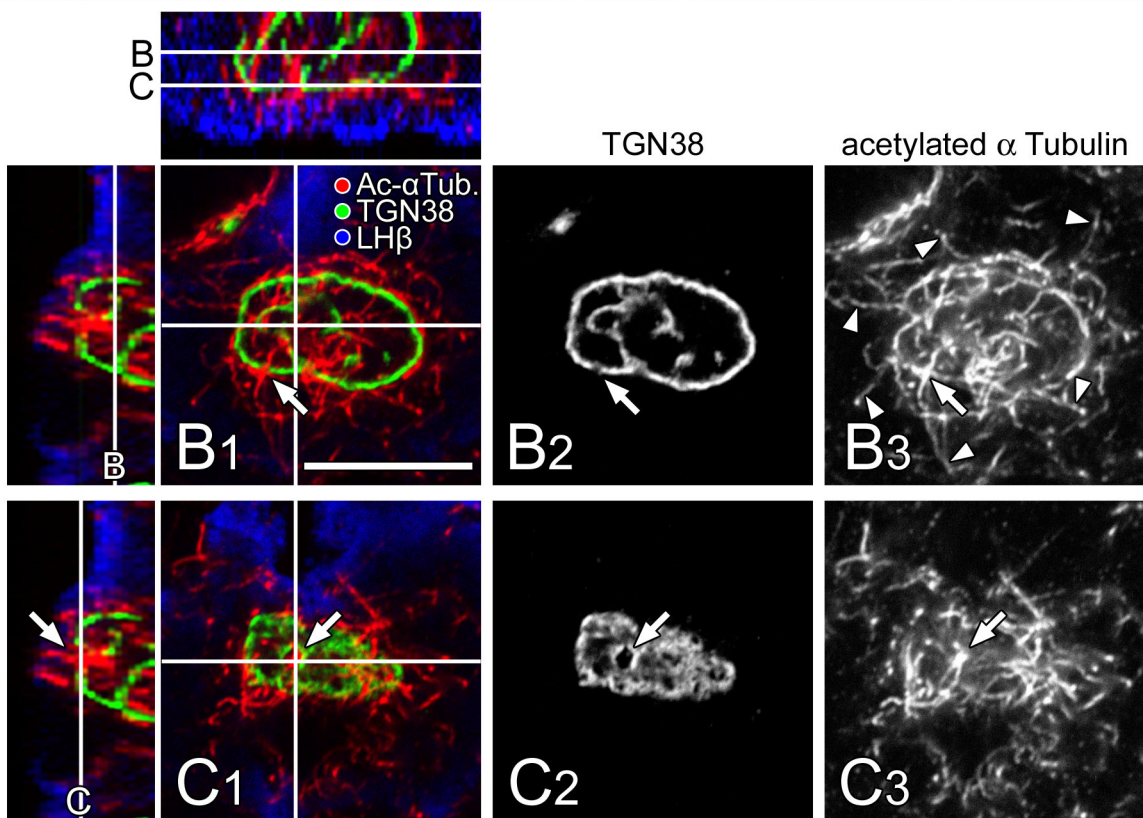
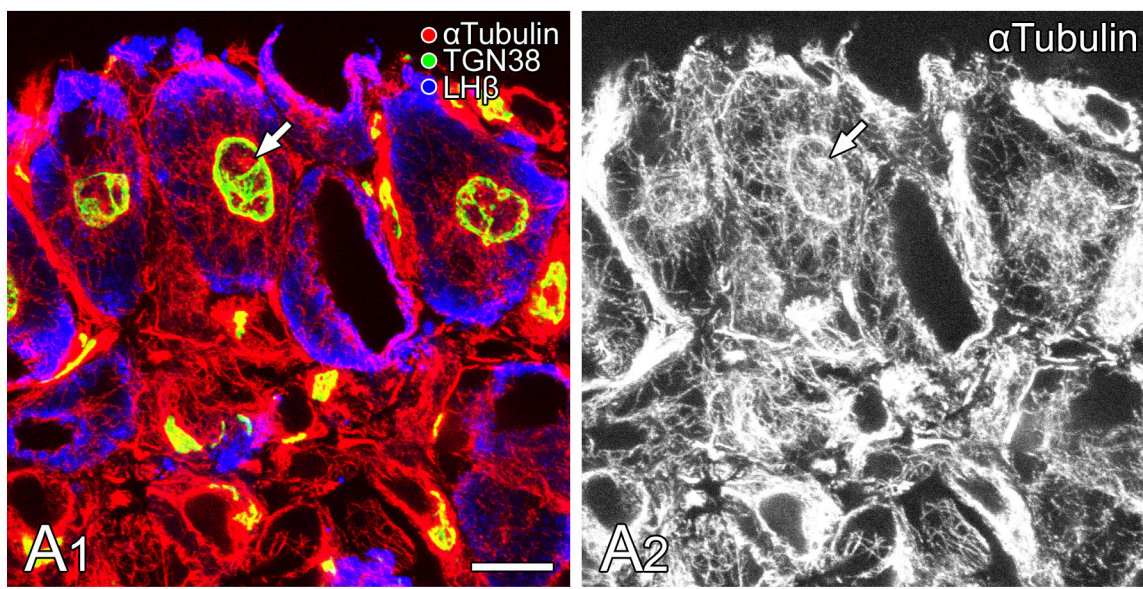
Watanabe et al., Fig. 3



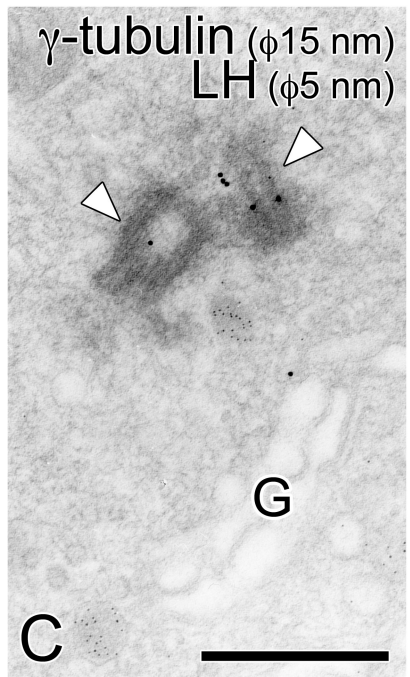
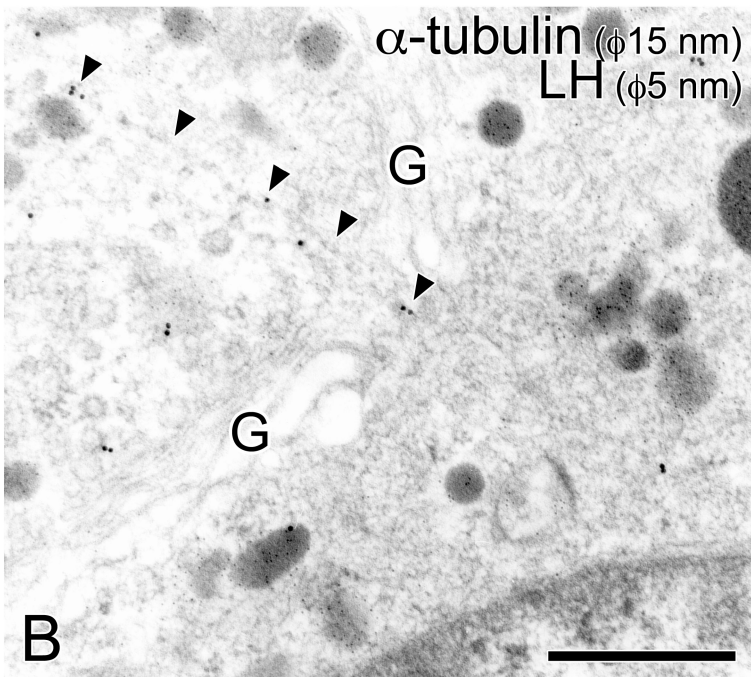
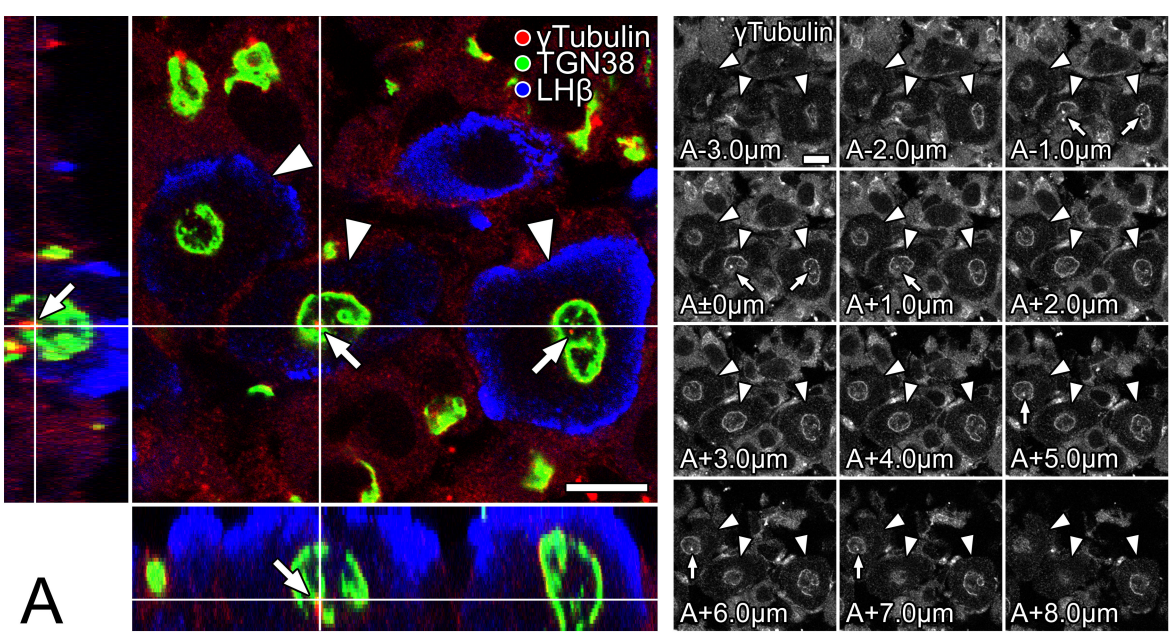
Watanabe et al., Fig. 4



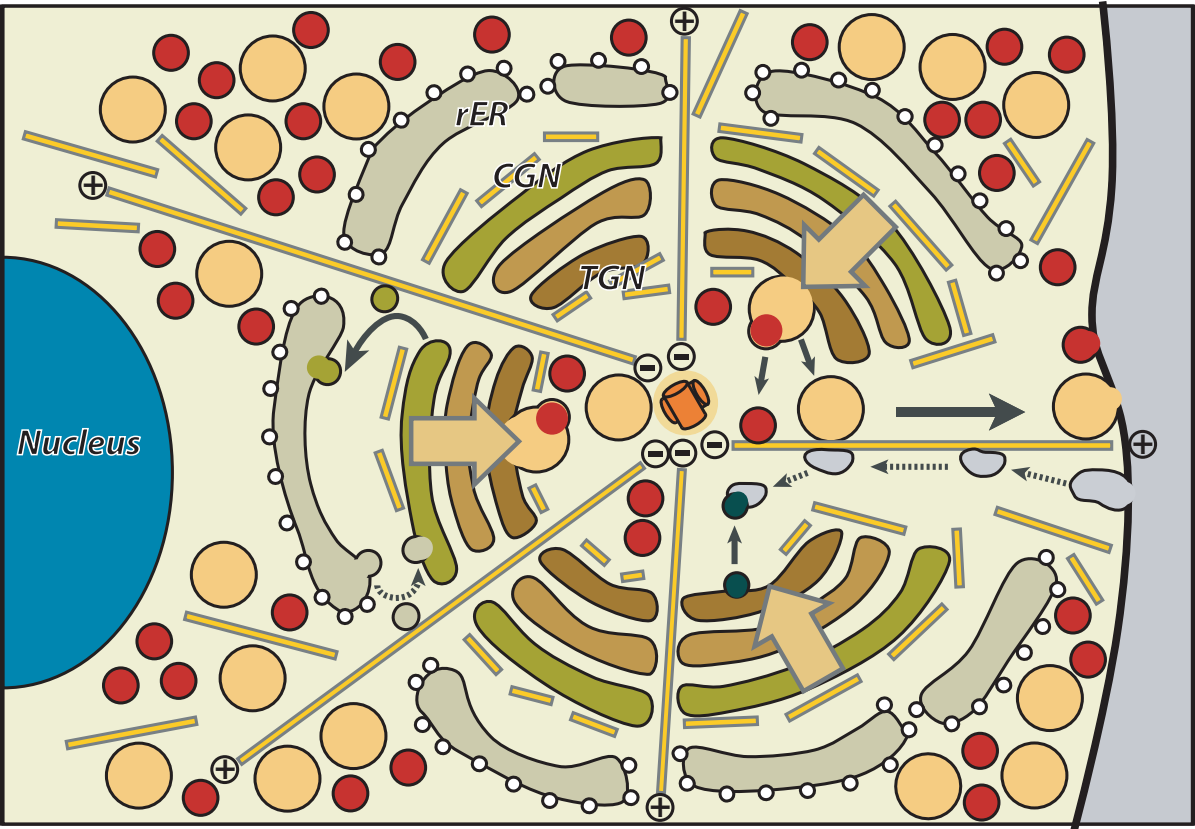
Watanabe et al., Fig. 5
















Watanabe et al., Fig. 6

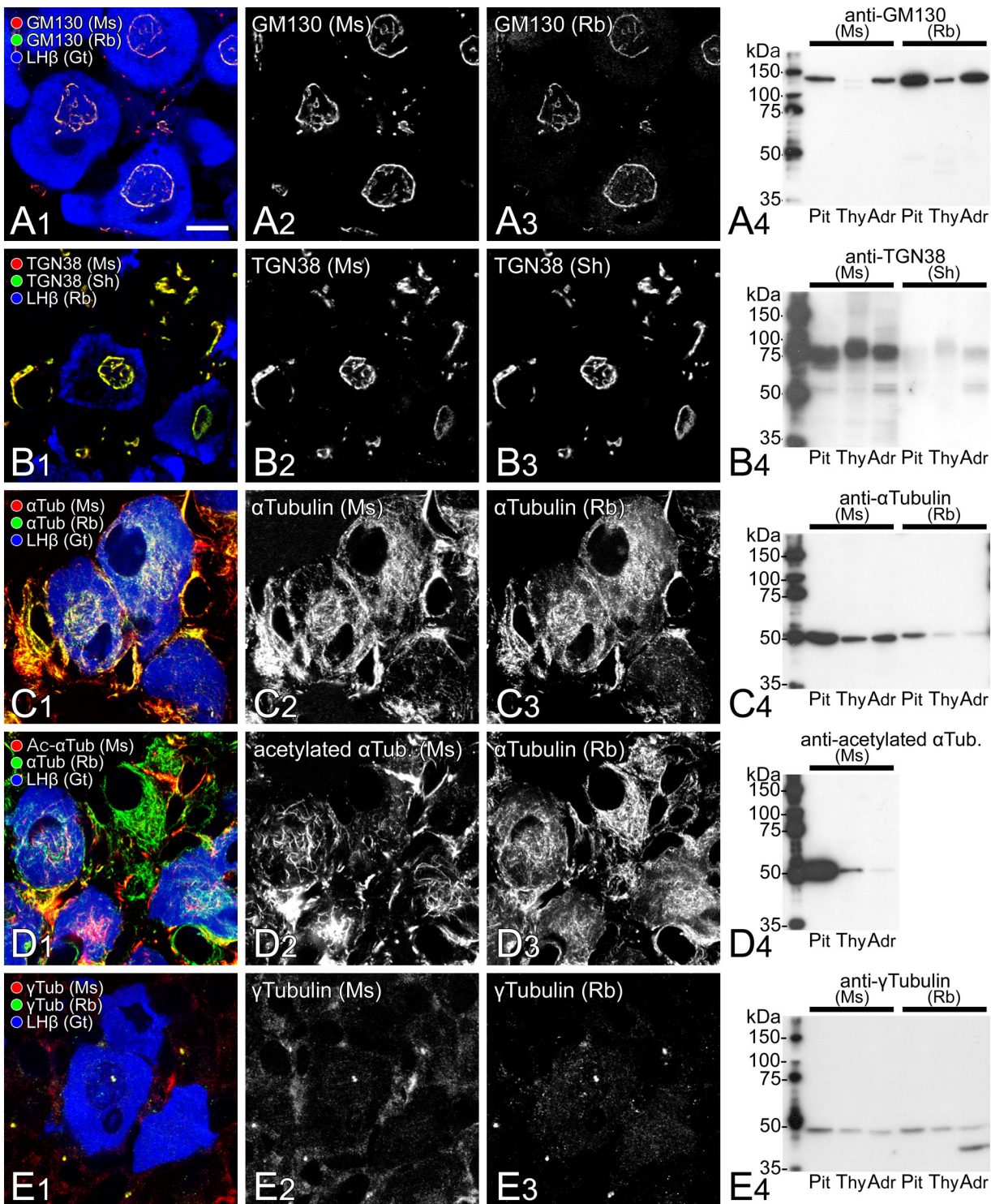


Watanabe et al., Fig. 7



-  microtubule
-  minus end of microtubule
-  plus end of microtubule
-  dynein-dependent movement
-  kinesin/KIFs - dependent movement
-  centrosome (γ tubulin positive)
-  flow of secretory proteins
-  COP I vesicle
-  COP II vesicle
-  secretory granule (CgA positive)
-  secretory granule (SgII positive)
-  primary lysosome
-  endosome
- rER*: rough endoplasmic reticulum
- CGN*: cis-Golgi network
- TGN*: trans-Golgi network

Watanabe et al., Fig.8



Watanabe et al., Supplementary Fig. 1